Published in final edited form as:
Adv Drug Deliv Rev. 2011 September 10; 63(10-11): 876–885. doi:10.1016/j.addr.2011.05.020.

Advances in Lymphatic Imaging and Drug Delivery

Satish K. Nune[a], **Padmaja Gunda**[b], **Bharat K. Majeti**[c], **Praveen K. Thallapally**[a], and **M. Laird Forrest**[b,*]

[a]Energy and Environment Directorate, Pacific Northwest National Laboratory, Richland, Washington 99352

[b]Department of Pharmaceutical Chemistry, University of Kansas, Lawrence, Kansas 66045

[c]Moores UCSD Cancer Center, University of California, San Diego, CA, 92093-0803

Abstract

Cancer remains the second leading cause of death after heart disease in the US. While metastasized cancers such as breast, prostate, and colon are incurable, before their distant spread, these diseases will have invaded the lymphatic system as a first step in their progression. Hence, proper evaluation of the disease state of the lymphatics which drain a tumor site is crucial to staging and the formation of a treatment plan. Current lymphatic imaging modalities with visible dyes and radionucleotide tracers offer limited sensitivity and poor resolution; however, newer tools using nanocarriers, quantum dots, and magnetic resonance imaging promise to vastly improve the staging of lymphatic spread without needless biopsies. Concurrent with the improvement of lymphatic imaging agents, has been the development of drug carriers that can localize chemotherapy to the lymphatic system, thus improving the treatment of localized disease while minimizing the exposure of healthy organs to cytotoxic drugs. This review will focus on the use of various nanoparticulate and polymeric systems that have been developed for imaging and drug delivery to the lymph system, how these new devices improve upon current technologies, and where further improvement is needed.

Keywords

drug delivery; polymeric carriers; lymphatic system; sentinel lymph nodes; quantum dots; dendrimers

1. Introduction

The lymphatic system is a complex network of nodes, vessels and thin-walled capillaries that drain the protein-rich lymph, excess fluids, and waste products from the extracellular space within most organs to the vascular system. The lymphatic system represents one of the chief components of the immune system, filtering potential immunogens from the extracellular space. The lymphatic system is not easily accessible by conventional modes of chemotherapeutic delivery, thus limiting the drug that reaches the lymphatic tissues. Discoveries in the past decade relating to lymphatic development and vessel growth (lymphangiogenesis) have provided new insights into the roles of lymphatic development and function in cancer progression.[1] Therefore lymphatics have been exploited as a potential route for the delivery of biologically active molecules.

*Dr. M. Laird Forrest, Department of Pharmaceutical Chemistry, 2095 Constant Avenue, University of Kansas, Lawrence, KS, 66047 USA, mforrest@ku.edu, Tel: 785 864 4388, Fax: 785 864 5736.

The lymphatic system is active in the metastatic spread of cancer and dissemination of infection. The regional lymph nodes, once invaded by tumor cells, act as a reservoir where cancer cells take root and seed into other parts of the body. However, due to the complexity, peculiar nature and anatomy of the lymphatic system, localization of drugs in the lymphatics is difficult. The recent findings by the Laakonen et al. have demonstrated that the tumor lymphatics carry specific markers that may be utilized to specifically target chemotherapeutics to the tumor lymphatics.[2] Various modes of drug delivery have been documented in the literature ranging from emulsions to nanoparticle capsules, which are complimented by various routes of administration including intramuscular, subcutaneous, oral and intraperitoneal.

2. Lymphatic Imaging

There is signifincant interest in the development of imaging methods to accurately map the drainage of solid tumors through the lymph nodes, specifically the sentinel lymph node (SLN).[3] The sentinel lymph node is considered the first lymph node or group of nodes reached by metastasizing cancer cells from the solid tumor, and the probability of finding the metastatic tumor cells is more likely compared to other lymph nodes. Cabanas *et al* in the year 1977 introduced the term sentinel node for the first time based on his work on penile cancer.[4] Since then, mercury injections, dyes and radioactives isotope have all been employed to visualize the lymphatic drainage of solid tumors.

Numerous clinical studies have emerged in last 10 years validating of the use of the sentinel node mapping in cancer staging and treatment. Morton *et al* reported in 1992 on the development of lymphatic imaging for the mapping of early stage melanoma using vital dyes, assuming in their studies that the sentinel node was primarily responsible for the dissemination of metastatic disease[5]. Giuliano *et al* quickly extended the use of vital dyes for breast cancer, reporting the first use of dyes for mapping lymphatic metastasis in breast cancer.[6] Turner *et al* in 1997 examined whether the sentinel node is required for dissemination of auxiliary metastasis in breast carcinoma.[7] They showed that if the sentinel node is free of cancer cells as determined by hematoxylin and eosin staining (H&E) and cytokeratin immunohistochemical staining (IHC), the probability of nonsentinel node involvement is less than 0.1 %, clearly demonstrating that the status of the sentinel lymph node is highly predicative of metastatic potential in breast carcinoma.

2.1 Non Invasive Techniques

Due to the complex and tortous morphology of the lymphatic system, it is a challenge for the physician to assess the pathology of the lymph system. For long time, the bipedal lymphography was the primary imaging technique for imaging lymphatics. However the advancement in the non-invasive techniques such as ultrasound (US), computer tomography (CT) or magnetic resonance imaging (MRI), fluoresence imaging has enabled the accurate evaluation of lymph nodes.[3e] These techniques have been enhanced by advancements in contrast angents for lymphatic imaging. Newer contrast agents are relatively non toxic compared to the first generations and exhibit high contrast with high site specificity even at very low concentrations.

2.1.1 Lymphoscintigraphy—Lymphoscintigraphy is a nuclear imaging method that uses radionuclide injections to obtain information about the lymphatic drainage. Lymphoscintigraphy is generally performed by subcutaneous injection of radiolabelled agents such as ^{99m}Tc-Labeled dextran,[8] ^{99m}Tc-Labeled human serum albumin[9] or ^{99m}Tc-Labeled sulfur colloid[10] that emit gamma rays. The main limitations associated with the lymphoscintigraphy are poor spatial resolution not allowing determination of the exact anatomic location of sentinel nodes and the short half-life of ^{99m}Tc (6.01 hours) that

necessitates onsite generation capabilities. To overcome the drawbacks associated with tradition lymphoscitigraphy, hybrid SPECT/CT imaging has been developed to obtain images with better contrast and resolution.[11] However, for routine preoperative sentinel biopsy, hybrid SPECT/CT is limited by the high associated cost.

2.1.2 Computer Tomography—X-ray computer tomography (CT), is a commonly used diagnostic imaging tool offering broad availability and relatively modest cost. X-ray CT is used to visualize tissue density differences that provide image contrast by X-ray attenuation between soft tissues and electrondense bone. It is desirable to enhance the contrast of diseased tissue with the use of X-ray contrast agents to increase the contrast between normal and cancerous tissue.[12] CT is a diagnostic method that is routinely performed to identify tumors prior to surgery for various cancers such as breast cancer. CT lymphography with excellent spatial and temporal resolution is commonly used to visualize the tumoral status and lymphatic drainage pathways. Currently, highly water soluble small organic iodinated molecules (e.g. iopamidol, ioversol, iohexol, and ioxaglate) are typically used as CT contrast enhancers for sentinel node imaging. Exposure of the patient to the ionizing radiation and the limited ability to obtain real time images remain significant challenges associated with this technique. Sentinel lymph node mapping using CT is primarily based on discerning anatomic characteristics such as size.

Suga *et al* investigated the use of computed tomographic lymphography (CT-LG) using the low molecular weight iodinated constrast agent iopamidol for visualizing breast lymphatic pathways.[13] Breast tumors are considered to disseminate through the lymphatic system, and the tumoral status of the sentinel node is reflective of the entire lymphatic system. In Suga's study, 0.5 and 1 mL of iopamidol were injected subcutaneously into 10 female dogs.[13b] By using CT, they were able to clearly visualize the direct connection of the sentinel node (first lymph node) and the lymphatic vessels with a maximum CT attenuation of 269±137 HU, even with 0.5 mL of iopamidol. They also performed CT-LG with 2 mL of iopamidol in five female volunteers, resulting in the localization of iopamidol in the sentinel node with a maximum attenuation of 269±137. The authors did not observe any significant adverse effects. Encouraged by these results, they also investigated the ability of CT to correctly localize the sentinel nodes by injecting 17 pateints with 2 mL iopamidol into peritumoral and periareolar areas (Fig 1).[14]. For comparison peri-operative blue-dye injections were also performed. The preoperative CT-LG provided accurate mapping of sentinel node and further drainage by the visualization of direct connection between a sentinel node and its afferent lymphatic vessels.

Recently, Takahashi *et al* studied the identification of sentinel nodes in breast cancer patients using subcutaneous injections to the tumor, the areola, or both, with CT-LG.[15] The sentinel nodes were correctly identified in 212 of 221 procedures (96 %) using CT-LG whereas dye-guided procedures yielded an idenfication rate of 92 % (202/219). They also compared the combined identification of sentinel nodes in breast cancer using CT-LG and the dye-guided method, and they investigated the relationship between sentinel node identification rates and clinicopathological findings. CT-LG, the dye-guided method, and the combined modalities showed no differences as a function of age, menopausal status, tumor diameter, or histopathological type. However, they found that identification rates were lower in the case of the dye-guided method in patients with a body mass index BMI of 25 or more, whereas the CT-LG and the combined methods were not influenced. The results obtained by Takahashi *et al* on the use of the combined method (CT-LG and dye-method) of identification of sentinel nodes in breast cancer are corroborated by a study conducted by Wu *et al* on the identification of sentinel lymph nodes in the tounge VX2 carcinoma model.[16] The main concern with the use of highly water soluble small organic iodinated

molecules as CT contrast enhancers is they tend to suffer from very short imaging times due to rapid renal clearance and non-specific vascular permeation.

2.1.3 Magnetic Resonance Imaging (MRI)—MRI is one of the most powerful noninvasive medical imaging techniques that is commonly used in clinical medicine. MRI is used to visualize the structure and health of tissues, and generally provides increased contrast between soft tissues compared to computer tomography (X-ray CT). MRI is based on the behavior, alignment and interaction of protons in the presence of an applied magnetic field. Within a strong magnetic field, protons in the tissue are perturbed from B_0; contrast agents are used to alter longitudinal (T1) or transverse (T2) relaxation times, which can be monitored by MRI. Contrast agent efficiency is determined by its relaxivity over a range of concentrations. Unlike radionuclide-based imaging, MRI eliminates the radiation dose and can offer higher spatial resolution.

Various contrast agents including nanoparticles have been developed to improve contrast in MRI imaging of lymphatic system;[17] these include, gadolinium based agents such as gadolinium-diethylenetriamine pentaacetic acid (Gd-DTPA), various iron oxide nanoparticles, and liposomes and dendrimers containing Gd(III) /or iron oxides. Significant benefits associated with iron oxide nanoparticles are their biocompatibility and ready detection at moderate to low concentrations. Super paramagnetic iron oxide nanoparticles (SPIONs) have a high saturation magnetization and loss of magnetization in the absence of magnetic field, and these nanoparticles are perceived to be relatively less toxic than optical imaging agents such as quantum dots.[18] Peptides, antibodies, proteins, and small molecules have been conjugated to SPIONs and cross linked iron oxide (CLIOs) for active targeting (REFs). Wunderbaldinger *et al.* used dextran-SPION to detect lymph node metastases in an experimental murine model using contrast-enhanced MRI.[19] Ultra small superparamagnetic iron oxide (USPIO) (Sinerem, Combidex, Clariscan) are particles with median diameter less than 50nm have been used as MRI contrast agents that may improve the ability of Magnetic Resonance Imaging (MRI) to see lymph nodes. USPIO nanoparticles have long serum half-lives, which is very important for systemic lymph node imaging.[20] The non-magnetic nature of USPIO in the absence of an external field benefits their use for imaging fine structures such as the lymphatics, as magnetism induced agglomeration is avoided.

Harisinghani *et al* investigated the use of highly lymphotropic superparamagmetic nanoparticles as contrast enhancers for noninvasive high resolution MRI detection of lymph-node metastasis in prostate cancer.[21] In a study of 33 patients, MRI images obtained in patients injected with lymphotropic superparamagmetic nanoparticles as contrast enhancers (2.6 mg of iron per kilogram of body weight) identified patients with nodal metastases with significantly higher sensitivity than conventional MRI (90.5 % vs. 35.4 %) and with improved diagnostic specificity 97.8 %. [21] Ross *et al* also successfully identifed lymph node metastases in prostate cancer using an intravenous infusion of ferumoxtran-10 (2.6 mg Fe/kg), a constrast agent specific to the lymph nodes.[22] Heesakkers *et al* further studied lymph node metastases in patients with prostate cancer outside the routine pelvic lymph node dissection area with enhanced MR-imaging using ferumoxtran-10 as contrast enhancer.[23] In their studies in patients having histopathological conformation of lymph node metastasis, MR lymphography images predominantly demonstrated the nodes outside the routine pelvic lymph node dissection over the CT-guided biopsy. Harisinghani *et al* in his recent findings reported that the use of ferumoxtran-10 as contrast enhancer with a sensitivity of 100 % and the specificity of 96% in patients with nodal involvement in prostate cancer.[24] Bellin *et al* reported the use of USPIO for malignant lymph node detection in 30 patients with urological and pelvic cancers with a sensitivity of 100 % and 80 % selectivity with no adverse side-effects.[25] Guimaraes *et al* recently reported the

sensitivity of 100 % and specificity of 95.7 % in 9 patients accessing lymph nodes in renal cell cancer using ferumoxtran-10 (Combidex).[26]

Axillary lymph node status has proven to be one of the most prognostic factors in breast cancer staging and survivorship. [27]The nodes are currently evaluated by surgical dissection followed by microscopic histological and immunohistological evaluation, which is destructive and can lead to serious complications. Murray *et al* used dynamic gadopentetate dimeglumine (Gd) enhanced MRI for non-invasive staging of the axillary lymph nodes in 47 women with a new primary breast cancer. Enhancement indices and nodal area were compared with histopathology of excised nodes. MRI images of axillary lymph node revealed the enhancement index of >21% and a nodal area of >0.4 cm^2 in 10 patients having auxillary metastases confirmed pathologically with a sensitivity of 100%, although the specificity was only 56 %.[28] Michel *et al* studied preoperative assessment of breast axillary lymph nodes by MR imaging using ultrasmall superparamagnetic iron oxide (USPIO) in 20 patients.[29] No serious adverse effects occurred in patients given a slow drip infusion (2.6 mg of iron per kilogram of the body weight, diluted to 100 ml saline]. A recent study by Kimura *et al* used USPIO lymphography to differentiate normal and diseased nodes by enhancement patterns based on the T2*-weighted and T1-weighed images.[30]

2.1.4 Optical Imaging—Optical imaging has the benefits of being non-invasive with good resolution at shallow depths and does not require any radiation exposure. Although various probes have been used in the sentinel lymph node optical imaging, this review emphasizes the use of quantum dots. Quantum dots (QDs) are fluorescent semiconductor nanocrystals (1 to 100 nm) with unique optical and electrical properties.[31] Compared to organic dyes and fluorescent proteins, QDs possess near-unity quantum yields and much greater brightness than most dyes (10–100 times). QDs also exhibit broad absorption characteristics, a narrow line width in emission spectra, continuous and tunable emission maxima due to quantum size effects, a relatively long fluorescence lifetime (5 to > 100 ns compared to 1–5 ns for organic dyes), and negligible photobleaching over minutes to hours (100–1000 times less than most fluorescent dyes). Synthetic techniques exist for the precise control of QD size and composition, which in large part control the absorption and emission characteristics. Furthermore, the surface of QDs can be functionalized with polyethylene glycol and other polymeric coatings that allow targeting and avoidance of macrophage clearance.[32] This can allow researchers to exploit QDs' unique properties for applications such as cell labeling, biosensing, and nucleic acid detection. QDs are increasingly used as fluorophores for *in vivo* fluorescence imaging.[33] Fluorescence imaging has several advantages compared to other imaging modalities since this method has good sensitivity and is non-invasive in nature using readily available and relatively inexpensive instruments. Also, fluorescence imaging has high resolution and sensitivity compared to radiotracers and dye absorption. A wide variety of *in vivo* studies have validated the potency of QDs.

Identification of lymph node drainage using QDs was one of its first applications along with mapping the reticuloendothelial system. QDs due to its size undergo endocytosis in cells particularly by macrophages in lymph node leading to the localization of QDs in sentinel lymph node enabling for fluorescence imaging. One important point to be noted is due to the localization of QDs at sentinel nodes, QDs may not be very good for mapping lymphatic drainage distal to the sentinel node. Ballou *et al* in 2004 studied the localization of four QDs with different surface coatings and demonstrated that the QDs remained fluorescent for at least four months *in vivo* and that the localization of QDs was dictated by the surface coating.[34] The authors recently extended this technique to mouse tumor models for sentinel lymph node imaging (Fig 2).[35] They studied the migration quantum dots bearing differently charged surface groups injected into murine tumor models to map sentinel lymph nodes. The authors used 655-nm emitting Zns-CdSe and 800-nm emitting ZnS-CdSe-CdTe

core QDs coated with an amphiphilic polymer having a very high density of surface carboxy groups, which were further modified with PEGs having terminal methoxy, carboxy, oramino functional groups; thus, generating PEG containing neutral, positive, and negatively charged QDs. Their fluorescence imaging studies on mice bearing m21 melonoma and MH-15 teratocarcinoma injected with significantly different sized QDs [hydrodyanamic diameters (nm); 22.6 (neutral), 30.4 (negative) and 41.2 (positive)] revealed to their surprise that all three QDs migrate similarly to lymph nodes, and charge and size had no effect drainage to surrounding lymph nodes.

Recently, Kobayashi used multiple QDs with similar physical sizes but different emission spectra to perform multispectrum imaging of lymphatic drainage. They employed five carboxy terminated QDs made of Cd-Se [565, 605, and 655 nm emission peaks] or CD-Te [705 and 800 nm emission peaks] (Table 1, Fig 3). Using different injection sites for each QD, they simultaneously visualized five separate lymphatic drainage pathways. This method has significant advantages over other techniques such as X-ray lymphangiography and MR-LG or radio nucleotide scintigraphy in cases where multiple drainage basins are examined simutaneously.[36] Recently Bhang *et al* developed a stable, size tunable (50–120 nm) hyaluronic acid-QD conjugate by using a simple electrostatic coupling method. The conjugates were used to demonstrate the fluorescence staining of lymphatic vessels *in vitro* and *in vivo*.[37] Robe *et al* reported the use of Cd/Se/Zns core shell QDs emitting around 655 nm for axillary lymph node mapping. Subcutaneous injection of 20 μL of a 1-μm QDs solution in the anterior paw of healthy nude mice lead to the localization of QDs in the axillary lymph nodes, with a maximum amount detected after 60 min, 2.42 % of the injected dose.[38]

Compared with other recently developed techniques for lymphatic imaging, fluorescence probes offer cost effectiveness, greater speed, and improved sensitivity at least for lymph nodes that are close enough to the surface to be imaged. For mapping deep nodes, the combination of QD fluorescence and other non-invasive techniques such as MRI or radiotracer scintigraphy would give more information about SLN than single techniques alone, such as ^{99m}Tc and dye injections. The use of simultaneous multicolor imaging may be particularly useful for tumor diagnosis; sentinel nodes could be imaged with non specific QDswhile and QDs with tumor specific ligands could be used to localize metastases in lymph nodes. Although the use of QDs for in vivo imaging offer advantages over other traditional techniques, there synthesis requires heavy metals, which raises questions about their safety and ultimately may impact their acceptance by regulatory agencies.[18b] [39]

3 Carriers for Lymphatic Imaging and Drug Delivery

There is a significant interest in the development of carrier systems for the targeted localization of contrast agents at lymph nodes.[40] Various factors such as size, composition, dose, surface charge, and the molecular weight of carriers influence the uptake by the lymphatics. For example there is an optimum range for lymphatic uptake of subcutaneously injected particles; particles greater than 100 nm in diameter will remain largely at the injection site, and particles between 10–80 nm are taken up well by the lymphatics, while smaller particles are absorbed by the capillary network that drains into the systemic circulation.[41] The use of nanocarriers based imaging agents has advantages such as size tunability and the surface of particles can be functionalized for improved selectivity, which may decrease toxicity due to less uptake by non-target tissues and organs.

3.1 Dendrimers

Dendrimers are well-defined, highly branched molecules that are synthesized with precise structural control and low polydispersity.[42] Recently dendrimers have emerged as versatile

materials for biomedical research applications such as drug delivery and imaging.[43] Dendrimers are promising materials for the development of imaging contrast agents due to precise control of their molecular structure, tunable variation in size, availability of a large number of reactive sites, low viscosity compared to equivalent molecular weight linear polymers, narrow polydispersity, and interior void space. By taking advantage of the regular structured nature of dendrimers, many of the obstacles associated with low molecular weight contrast agents and imprecise synthetic polymers can be overcome. The two major strategies commonly employed in the synthesis of dendrimers are the “divergent” and “convergent” methods. The divergent method, introduced by Tamalia *et al*., begins with a multifunctional core followed by repeated addition of monomers to increase molecular weight and exponentially increase surface termini.[44] By contrast, the convergent method pioneered by Frechet *et al.* begins from the surface and proceeds inward to a multivalent core where the dendrimer segments are joined together.[45] Biocompatible water soluble dendrimers such as polyamidoamine (PAMAM, i.e. Starburst™), internal architectures nearly mimicking the structure of proteins and peptides, have have gained attention for bio-imaging applications.

The utilization of dendrimer-based contrast agents for dynamic magnetic resonance lymphangiography was pioneered by Kobayahsi *et al* in 2003.[46] Gd-containing dendrimers with different sizes and molecular structures (PAMAM-G8, PAMAM-G4, and DAB-G5) [PAMAM: polyamido amine, DAB: diaminobutyl] were conjugated with Gd and compared as constrast agents. Size and molecular structure had large impacts on distribution and pharmacokinetics. For example, PAMAM-G8 had a relatively long life in the circulartory system when injected intravenously with minimum leakage out of the vessels, whereas PAMAM-G4 was cleared rapidly from the systemic circulation due to rapid renal clearance but had immediate survival in lymphatic circulation. The smaller sized DAB-G5 accumulated and was retained in that lymph nodes, which may be useful for lymph node imaging using MR-LG. Gadomer-17 and GD-(DTPA)-dimeglumine (Magnevist) were compared as controls. Imaging experiments revealed that all of the reagents are able to visualize the deep lymphatic system except GD-(DTPA)-dimeglumine. PAMAM-G8 was best suited to visualize the lymphatic vessels whereas DAB-G5 was best able to visualize lymph nodes. The behavior of PAMAM-G4 was in between that of PAMAM-G8 and DAB-5, providing good contrast of both the nodes and connecting vessels. Gadomer-17 was able to visualize lymph nodes, but not as clearly as Gd-based dendrimers.

Kobayashi also investigated the delivery of various Gd-PAMAM (PAMAM-G2, G4, G6, G8) and DAB-G5 dendrimers to the sentinel lymph nodes and compared its visualization with other nodes.[47] The G6 dendrimer was found to be absorbed and retained in the lymphatic system and was able to provide excellent opacification of sentinel lymph nodes.[47] Talanov *et al* recently introduced the bifucntional dendrimers-based nanoprobe for dual modality magnetic resonance and fluorescence imaging (MR-FI).[48] PAMAM dendrimers were covalently conjugated to GD-DTPA chelates and the NIR fluorescent dye, Cy 5.5. To our knowledge this is the first dual imaging probe that provides excellent spatial resolution of MRI with very high sensitivity of fluorescence. Using G6-PAMAM-Gd-Cy the sentinel nodes were more clearly observed using a combination of MRI and fluorescence demonstrating the potential of the dendrimers as platform for dual imaging. For consistent visualization of the sentinel lymph nodes, 25 mL of 30 mM Gd-G6PAMAM-Cy 5.5 (750 nmol based on Gd) was required. The low sensitivity associated with MRI imaging by Gd-G6PAMAM necessitates high doses of contrast agent, and the early QD studies used fluorophores with limited depth penetration and potential heavy metal toxicity., Kobayashi *et al* further extended the simultaneous use of two modalities (radionuclide and optical imaging) to overcome the sensitivity limitation and depth limitations of with each individual method. They developed multimodal nano probes for radionuclide and multicolor optical lymphatic imaging using G6-PAMAM dendrimers conjugated with near infared (NIR) dyes

and an ^{111}In radionuclide probe[49]. In the head and neck region of mice, the radionuclide provided semi-quantitative information of delivery whereas the optical probes provided the qualitative information with excellent spatial resolution. Kobayashi further proposed the use of two nanomaterials for multicolor imaging of lymphatic system -- quantum dots for labeling cancer cells and dendrimer based optical agents for visualization of lymphatic drainage and identification of sentinel lymph nodes.[50] Based on the developments, it is very apparent that no imaging modality is perfect; every method has its own advantages and limitations on the visualization of complex lymphatic system.

Polylysine coated dendrimers have been used to target the lymphatic system and lymph nodes. Porter and co-workers demonstrated that PEGylated poly-L-lysine dendrimers are well absorbed from subcutaneous injection sites and that the extent of lymphatic transport may be enhanced by increasing the size of the PEGylated dendrimer complex. They evaluated the lymphatic uptake and lymph node retention properties of several generation four dendrimers capped with PEG or 4-benzene sulphonate after subcutaneous administration in rats. Three types of PEGs with molecular weights of 200, 570, or 2000 Da were used for the surface modification. PEG200 derived dendrimers were quickly and completely absorbed into the blood when injected subcutaneously and only 3% of the administered dose was observed in the pooled thoracic lymph over 30 hrs. Absorption of PEG570 and PEG 2000 derived dendrimers in blood was low and a higher amount was recovered in lymphatics (ca. 29%) over 30 hrs. After intravenous administration, indirect access to the lymph was observed for PEG 570 and PEG 2000 because of equilibration across the capillary beds with the lymph. However, the benzene sulphonate capped dendrimer was not well absorbed either in blood or in lymph following subcutaneous inejction.[51]

3.2 Polymeric Carriers

Numerous polymeric particles have been synthesized for targeted and sustained drug delivery. The polymers are either natural polymer like Dextran, alginate, chitosan, gelatin and Hyaluronic acid or synthetic polymers like PLGA, PLA and PMMA.

3.2.1 Natural Polymers—Owing to its excellent biocompatibility, dextran has been used as a carrier for drug molecules, peptides, proteins and enzymes. Kim *et al* reported the synthesis of Cyclosporine A loaded dextran acetate particles labeled with ^{99m}Tc. These particles were prepared by reacting dextran with acetic anhydride followed by Cyclosoprine A loading. Upon subcutaneous injection into the foot pad of rats, these particles steadily distributed Cyclosporin A as well the ^{99m}Tc label throughout the lymph nodes.[52] A lymphotropic delivery system has been reported for mitomycin C by conjugating it to dextrans with average molecular weights of 10, 70, and 500 kDa. Following intramuscular injection in mice, the mitomycin C-dextran conjugates (MMC-D) were retained at the injection site for a longer period compared to free mitomycin C. Moreover, there was a significant accumulation of MMC-D in regional lymph nodes which persisted for nearly 48 h while the free mitomycin was rapidly cleared. The in vivo effect of MMC-D on lymph node metastasis was evaluated using a metastatic leukemia L1210 model in mice. There was a significant effect on the weight of lymph nodes when mice were treated with a 2.5 mg/kg dose of MMC-D (70 and 500 kDa) four days post-tumor inoculation, while free MMC and MMC-D (10 kDa) did not exert any effect.[53]

Hyaluronic acid, an anionic non-sulfated glycosaminoglycan, is a biocompatible polymer that follows **l**ymphatic drainage from the interstitial spaces. Cai *et al* synthesized a cisplatin hyaluronic acid conjugate for intralymphatic delivery of the drug. Upon subcutaneous injection into the upper mammary fat pad of female rats, the conjugate resulted in a

significant increase in the drug concentration in the local regional nodal tissue above the standard cisplatin formulation. Cisplatin-HA conjugates were well tolerated in rats without any major organ toxicity after 96 hrs. The conjugate also exhibited sustained release kinetics which would in turn lead to into lower organ over time.[54] The hyaluronate (HA) receptor has been used to deliver anticancer drugs selectively to lymph nodes and tumors. To investigate the specific distribution of HA into regional lymph nodes and to evaluate the HA receptor on lewis lung carcinoma cells, ^{14}C-labelled HA and fluorescent HA (FR-HA) were synthesized, along with drug conjugates HA-mitomycin C and HA-epirubicin. Upon s.c administration of ^{14}C-HA and HA-epirubicin, distribution of both compounds was observed in the lymph nodes. Cellular internalization studies showed that FR-HA was entered into the cells via CD44 receptors. When HA-mitomycin C (MMC) was injected into lewis lung carcinoma implanted mice at a low dose of 0.01 mg/kg, anti-metastasis effects were observed, whereas free MMC had no effect on metastasis in the same model.

3.2.2 Synthetic polymers—Biodegradable nanospheres of poly(lactide-co-glycolide) have been reported to deliver drugs and diagnostic agents to the lymphatic system. Sub-100 nm nanospheres were coated with block co-polymers of poloxamers and poloxamines, along with radiolabelled ^{111}In-oxine to trace the nanoparticles *in vivo*. Uptake of the block copolymer coated nanospheres in the lymphatic system was higher in comparison with the uncoated system upon s.c. injection. Moreover, a maximum uptake of 17% of the administered dose was observed in the regional lymph node.[55] Dunne *et al* used a conjugate of cis-diamminedichloro-platinum(II) (CDDP) and poly(ethylene oxide)-block-poly(lysine) (PEO-b-PLys) block copolymer for the treatment of lymph node metastasis. When VX-2 tumor bearing animals were treated with high drug-loaded (48 wt% CDDP) polymers, it resulted in 90% of the animals being cured. Limited tumor growth in the draining lymph nodes and prevention of systemic metastasis was observed with one animal treated with 10 wt% CDDP- polymer.[56]

Efficient delivery of anti-cancer agents to the lymph nodes or lymphatic vessels where tumor cells may metastasize is important to curb early and occult disease. Johnston and coworkers designed a biodegradable intrapleural (ipl) implantable drug delivery system consisting of a gelatin sponge impregnated with polylactide-co-glycolide paclitaxel (PLGA-PTX) to target thoracic lymphatics. This system showed sustained drug release properties *in vitro* and exhibited lymphatic targeting capability in rat models. Three types of formulations, a paclitaxel solution, PLGA-PTX microspheres, and a PLGA-PTX sponge were used to study the pharmacokinetics. For ipl sponge implantation, the PLGA-PTX sponge was placed into the pleural space through a left thoractomy. Substantial lymphatic drug exposure was observed (>400 fold) when PLGA-PTX (equivalent to Taxol 7 mg/kg) microspheres and PLGA-PTX (Taxol 7 mg/kg) sponges were placed within the pleural cavity compared to paclitaxel solution (Taxol 8 mg/kg) injected by iv or ipl. Histological experiments revealed the presence of these PLGA-PTX microspheres in lymphatic tissues upto 4 weeks after the sponge was implanted. The therapeutic effect of these particles was studied in an orthotopic lung cancer model with tumor resection 14 days post tumor cell implantation. Lymph node metastasis was examined in the animals after 32 days following ipl placement of the PLGA-PTX sponge, placebo sponge, or no treatment. The incidence of lymphatic metastasis and tumor burden was significantly lower in the treatment group compared with that of the non treatment controls and placebo sponge controls. Thirty-two of a total of 40 lymph nodes (80%) obtained from control animals (28 from no treatment controls and 12 from placebo sponge controls) were found to contain tumor metastases. Four of 26 lymph nodes (15.4%) from the treatment group showed tumor involvement, all of which were in the contralateral mediastinum.[57] Kumanohoso et. al developed a new drug delivery system by loading bleomycin (BLM) into a small cylinder of biodegradable polylactic acid (PLA) to target lesions. Bleomycin was continuously released for more than 3 weeks from the polymer in

saline. A higher concentration of BLM was observed in abdominal lymph nodes following s.c. implantation of BLM-PLA was than a s.c. injection of BLM-soln. Further, the anti-tumor effect of BLM-PLA was significantly higher compared to BLM-soln and no treatment.[58]

A new system for the delivery bleomycin (BLM) to target lesions was established by incorporating BLM into a small cylinder of a biodegradable colloidal particulate based nanoparticle carrier system to target thoracic lymphatics and lymph nodes. The lymphatic distribution of various nano and micro particles of charcoal, polystyrene; and poly(lactide-co-glycolide) was investigated after intrapleural implantation in rats. All three types of particles were cleared by regional thoracic lymphatic system following injection into pleural space. The lymphatic uptake was observed as early as 3 hrs after injection mainly through the parietal pleura. The most extensive lymphatic distribution was observed for particles of size 0.7–2 microns. One possible explanation given by the authors for the low uptake of small particles in lymph nodes is that, even though these particles may have easy access to pleural lymphatics, they fail to be retained in regional lymph nodes.[59]

3.3 Miscellaneous Carriers for Lymphatic Drug Delivery

Because of their unique mechano chemical properties, carbon nanotubes (CNT) are being investigated as drug carriers. They have a high surface area, mechanical strength, thermal and chemical stability making them versatile carriers for drugs, proteins, radiologicals, and peptides to target tumor tissues. Hydrophilic multi-walled carbon nanotubes (MWNT) decorated with magnetic nanoparticles (MN-MWNT) have been used to target the lymphatic system. MN-MWNTs were obtained by chemical co-precipitation of Fe^{2+} and Fe^{3+} onto the outer surface of polyacrylic acid grafted MWNTs (PAA-*g*-MWNTs). Upon subcutaneous injection of these particles into the left footpad of Sprague Dawley rats, the left popliteal lymph nodes were dyed black as early as 3 hrs after administration. Moreover, no uptake was observed in major internal organs such as the liver, spleen, kidney, heart, and lungs, throughout the whole course of the experiment, suggesting the preferential absorption of MN-MWNTs by lymphatic vessels and their subsequent transfer into lymph nodes. Lymphatic delivery efficiency of these particles was evaluated by loading them with gemcitabine (GEM). The animals were randomized into 5 groups: GEM without drug carrier and external magnetic field (GEM-Control); GEM loaded MN-MWNTs with external magnetic field (MN-MWNTs-GEM-Magnet), GEM loaded MN-MWNTs without magnetic field (MN-MWNTs-GEM), GEM loaded in MN-ACs (nano-sized activated carbon decorated with magnetic nanoparticles), GEM loaded in MN-ACs with magnetic field (MN-ACs-GEM-Magnet), and GEM loaded in MN-ACs without magnetic field (MN-ACs-GEM). The MN-MWNTs-GEM-Magnet group exhibited the highest concentration of gemcitabine in the lymph nodes throughout the experiment. A significant difference ($P < 0.01$) between MN-MWNT's and other control groups was observed at 6, 12, 24 and 192 hrs. Furthermore, MN-MWNTs showed a higher gemcitabine delivery efficiency than MN-ACs, especially when an external magnetic field was applied, which aggregated the MN-MWNTs at a specific location. In addition, the plasma concentration of gemcitabine distinctly decreased when loaded into MN-MWNTs.[60] McDevitt *et al* synthesized tumor-targeting CNT constructs by covalent attachment of multiple copies of tumor-specific monoclonal antibodies, radiometal-ion chelates, and fluorescent probes to sidewall-functionalized, water-soluble CNTs. The antibodies used were Rituximab and Lintuzumab. DOTA was used as a metal ion chelator while the fluorescent probe was fluorescein. CNT-([^{111}In]DOTA)(Rituximab) specifically targeted a disseminated human lymphoma *in vivo* experiments compared to the controls CNT-([^{111}In]DOTA)(Lintuzumab), and [^{111}In]Rituximab.[61]

The drug delivery efficiency of water-dispersed carbon nanohorns in a nonsmall cell lung cancer model has been evaluated by Tsuchida and coworkers. These nanohorns were

prepared by adsorption of polyethylene glycol-doxorubicin conjugate (PEG-DXR) onto oxidized single-wall carbon nanohorns (oxSWNHs). Intratumoral injection of PEG-DXR-bound oxSWNHs into mice bearing human non small cell lung cancer (NCI-H460) resulted in significant retardation of tumor growth. Histological analyses revealed migration of oxSWNHs to the axillary lymph node, which is a major site of breast cancer metastasis near the tumor, possibly by means of interstitial lymphatic-fluid transport.[62] Shimada *et al* reported a silica particle based lymphatic drug delivery system for anti-cancer agent, bleomycin. The drug was adsorbed on the surface of small silica (SI) particles and its therapeutic efficacy as compared to that of free bleomycin solution in a transplanted tumor model in animals. The inhibitory effect on tumor growth and lymph node metastasis was remarkable for Si particle adsorbed bleomycin compared to with free BLM solution.[63] Activated carbon particles have been used for adsorption and sustained release of aclarubicin (ACR-CH) into lymph nodes. ACR-CH resulted in significantly higher distribution of aclarubicin to the auxiliary lymph nodes compared to aqueous solution of the drug (ACR-sol) after subcutaneous administration into the fore foot-pads of rats. A lower uptake of aclarubicin was observed in other tissues with ACR-CH.[64] Activated carbon particles have also been used by another group for adsorption of aclacinomycin A, adriamycin, mitomycin C, and pepleomycin. Animal experiments demonstrated that the LD50 values for these carbon particle adsorbed drugs were higher than those of the drugs in solution. In addition, the lymph node concentration of the drugs was also maintained at a higher level in the new dosage form than in the solution form.[65]

4. Conclusion

The lymphatics lay a major role in the progression of cancer and the function of the immune system, and their proper function is crucial to health. The development of drug delivery systems and imaging agents that can directly treat disease advanced into the lymphatics and gauge the response to treatments in these tissues will improve patient diagnoses and treament. Lymphatic imaging has proven very important in the staging of cancers, and new imaging tools are making this a much less invasive process by reducing or eliminating the need for biopsies and unnecessary removal of healthy nodal tissue. In addition, newer imaging agents provide higer resolution and less risk to patients due to radiation and toxicity. Drug delivery to the lymphatics is in its infancies, but initial trials in animal models have show the tremendous potential this route of delivery has for the control and containment of early stage cancers. In summary, although lymphatic drug delivery and imaging will not replace systemic chemotherapy and more generalized tissue imaging tools, drug delivery and imaging agents designed specifically for the lymphatics will complement and enhance existing tools for the treament of cancer patients.

Acknowledgments

The authors thank the Pacific Northwest National Laboratory for Laboratory Directed Research and Development Fund (operated by Battelle for the U.S. Department of Energy under Contract DE-AC05-76RL01830), the American Heart Association, the NIH (R03 AR054035, P20 RR016443, R21 CA132033 and P20 RR015563), the NSF (CHE0719464), and the American Cancer Society (RSG-08-133-01-CDD).

References

1. Oliver G, Detmar M. Genes & Dev. 2002; 16:773. [PubMed: 11937485]
2. Laakkonen P, Porkka K, Hoffman JA, Ruoslahti E. Nature Medicine. 2002; 8:751.
3. a) Lohrmann C, Foeldi E, Langer M. Microvascular Research. 2009; 77:335. [PubMed: 19323976] b) Barrett T, Choyke PL, Kobayashi H. Contrast Media & Molecular Imaging. 2006; 1:230. [PubMed: 17191764] c) Clement O, Luciani A. European Radiology. 2004; 14:1498. [PubMed: 15007613] d) Choi SH, Moon WK, Hong JH, Son KR, Cho N, Kwon BJ, Lee JJ, Chung JK, Min

HS, Park SH. Radiology. 2007; 242:137. [PubMed: 17090719] e) Luciani A, Itti E, Rahmouni A, Meignan M, Clement O. European Journal of Radiology. 2006; 58:338. [PubMed: 16473489] f) Misselwitz B. European Journal of Radiology. 2006; 58:375. [PubMed: 16464554] g) Jaina, Ratnesh; Dandekara, P.; Patravale, V. Journal of Controlled Release. 2009; 138:90. [PubMed: 19445982]

4. Cabanas RM. Cancer. 1977; 39:456. [PubMed: 837331]
5. Morton DL, Wen DR, Wong JH, Economou JS, Cagle LA, Storm FK, Foshag LJ, Cochran AJ. Archives of Surgery. 1992; 127:392. [PubMed: 1558490]
6. Giuliano AE, Kirgan DM, Guenther JM, Morton DL. Annals of Surgery. 1994; 220:391. [PubMed: 8092905]
7. Turner RR, Ollila DW, Krasne DL, Giuliano AE. Annals of Surgery. 1997; 226:271. [PubMed: 9339933]
8. Henze E, Schelbert HR, Collins JD, Najafi A, Barrio JR, Bennett LR. Journal of Nuclear Medicine. 1982; 23:923. [PubMed: 6181235]
9. a) Ohtake E, Matsui K, Kobayashi Y, Ono Y. Journal of Nuclear Medicine. 1983; 24:P41.b) Nathanson SD, Anaya P, Avery M, Hetzel FW, Sarantou T, Havstad S. Annals of Surgical Oncology. 1997; 4:161. [PubMed: 9084854]
10. Eshima D, Eshima LA, Herda SC, Algozine CA, Burris TG, Vansant JP, Alazraki NP, Taylor AT. Journal of Nuclear Medicine. 1996; 37:327.
11. a) Uren RF. Annals of Surgical Oncology. 2009; 16:1459. [PubMed: 19363583] b) van der Ploeg IMC, Olmos RAV, Kroon BBR, Rutgers EJT, Nieweg OE. European Journal of Nuclear Medicine and Molecular Imaging. 2009; 36:6. [PubMed: 18712384] c) Ploeg IMCD, Olmos RAV, Kroon BBR, Nieweg OE. World Journal of Surgery. 2008; 32:1930. [PubMed: 18478289]
12. Yu SB, Watson AD. Chemical Reviews. 1999; 99:2353. [PubMed: 11749484]
13. a) Suga K, Ogasawara N, Okada M, Matsunaga N. Surgery. 2003; 133:170. [PubMed: 12605178] b) Suga K, Ogasawara N, Yuan Y, Okada M, Matsunaga N, Tangoku A. Investigative Radiology. 2003; 38:73. [PubMed: 12544070]
14. Suga K, Yuan Y, Okada M, Matsunaga N, Tangoku A, Yamamoto S, Oka M. Radiology. 2004; 230:543. [PubMed: 14699178]
15. Takahashi M, Sasa M, Hirose C, Hisaoka S, Taki M, Hirose T, Bando Y. World Journal of Surgical Oncology. 2008; 6
16. Wua H, Xu X, Ying H, Hoffman MR, Shen N, S Y, Zhou L. International Journal of Oral and Maxillofacial Surgery. 2009 (in Press).
17. a) Na HB, Song IC, Hyeon T. Advanced Materials. 2009; 21:2133.b) Hasebroock KM, Serkova NJ. Expert Opinion on Drug Metabolism & Toxicology. 2009; 5:403. [PubMed: 19368492] c) Waters EA, Wickline SA. Basic Research in Cardiology. 2008; 103:114. [PubMed: 18324367]
18. a) Mahmoudi M, Simchi A, Imani M, Milani AS, Stroeve P. Journal of Physical Chemistry B. 2008; 112:14470.b) Lewinski N, Colvin V, Drezek R. Small. 2008; 4:26. [PubMed: 18165959]
19. Wunderbaldinger P, Josephson L, Bremer C, Moore A, Weissleder R. Magnetic Resonance in Medicine. 2002; 47:292. [PubMed: 11810672]
20. a) Helbiech TH. Breast Cancer Research. 2008; 10b) McCauley TR, Rifkin MD, Ledet CA. Journal of Magnetic Resonance Imaging. 2002; 15:492. [PubMed: 11948841]
21. Harisinghani MG, Barentsz J, Hahn PF, Deserno WM, Tabatabaei S, van de Kaa CH, de la Rosette J, Weissleder R. New England Journal of Medicine. 2003; 348:2491. [PubMed: 12815134]
22. Ross, RobertW; Zietman, AnthonyL; Xie, Wanling; Coen, JohnJ; Dahl, DouglasM; Shipley, WilliamU; Kaufman, DonaldS; Islam, Tina; Guimaraes, AlexanderR; Weissleder, aRalph; Harisinghani, M. Clinical Imaging. 2009; 33:301. [PubMed: 19559353]
23. Heesakkers RAM, Jager GJ, Hovels AM, de Hoop B, van den Bosch HCM, Raat F, Witjes JA, Mulders PFA, van der Kaa CH, Barentsz JO. Radiology. 2009; 251:408. [PubMed: 19401573]
24. Harisinghani MG, Barentsz JO, Hahn PF, Deserno W, de la Rosette J, Saini S, Marten K, Weissleder R. Academic Radiology. 2002; 9:S312. [PubMed: 12188258]
25. Bellin MF, Roy C, Kinkel K, Thoumas D, Zaim S, Vanel D, Tuchmann C, Richard F, Jacqmin D, Delcourt A, Challier E, Lebret T, Cluzel P. Radiology. 1998; 207:799. [PubMed: 9609907]

26. Gulmaraes AR, Tabatabei S, Dahl D, McDougal WS, Weissleder R, Harisinghani MG. Urology. 2008; 71:708. [PubMed: 18295316]
27. Catzeddu T, Bertelli G, Del Mastro L, Venturini M. Journal of Surgical Oncology. 2004; 85:129. [PubMed: 14991884]
28. Murray AD, Staff RT, Redpath TW, Gilbert FJ, Ah-See AK, Brookes JA, Miller ID, Payne S. British Journal of Radiology. 2002; 75:220. [PubMed: 11932214]
29. Michel SCA, Keller TM, Frohlich JM, Fink D, Caduff R, Seifert B, Marincek B, Kubik-Huch RA. Radiology. 2002; 225:527. [PubMed: 12409591]
30. Kimura, Kosei; Tanigawa, N.; Matsuki, Mitsuru; Nohara, Takehiro; Iwamoto, Mitsuhiko; Sumiyoshi, Kazuhiro; Tanaka, Satoru; Takahashi, Yuko; Narumi, Y. Breast Cancer. 2009
31. Zhang H, Yee D, Wang C. Nanomedicine. 2008; 3:83. [PubMed: 18393668]
32. a) Dif A, Boulmedais F, Pinot M, Roullier V, Baudy-Floc'h M, Coquelle FM, Clarke S, Neveu P, Vignaux F, Le Borgne R, Dahan M, Gueroui Z, Marchi-Artzner V. Journal of the American Chemical Society. 2009; 131:14738. [PubMed: 19788248] b) Schipper ML, Iyer G, Koh AL, Cheng Z, Ebenstein Y, Aharoni A, Keren S, Bentolila LA, Li JQ, Rao JH, Chen XY, Banin U, Wu AM, Sinclair R, Weiss S, Gambhir SS. Small. 2009; 5:126. [PubMed: 19051182]
33. a) Gao XH, Cui YY, Levenson RM, Chung LWK, Nie SM. Nature Biotechnology. 2004; 22:969.b) Misra RDK. Nanomedicine. 2008; 3:271. [PubMed: 18510421]
34. Ballou B, Lagerholm BC, Ernst LA, Bruchez MP, Waggoner AS. Bioconjugate Chemistry. 2004; 15:79. [PubMed: 14733586]
35. Ballou B, Ernst LA, Andreko S, Harper T, Fitzpatrick JAJ, Waggoner AS, Bruchez MP. Bioconjugate Chemistry. 2007; 18:389. [PubMed: 17263568]
36. a) Kobayashi H, Hama Y, Koyama Y, Barrett T, Regino CAS, Urano Y, Choyke PL. Nano Letters. 2007; 7:1711. [PubMed: 17530812] b) Hama Y, Koyama Y, Urano Y, Choyke PL, Kobayashi H. Breast Cancer Research and Treatment. 2007; 103:23. [PubMed: 17028977]
37. Mang SH, Won N, Lee TJ, Jin H, Nam J, Park J, Chung H, Park HS, Sung YE, Hahn SK, Kim BS, Kim S. Acs Nano. 2009; 3:1389. [PubMed: 19476339]
38. Robe A, Pic E, Lassalle HP, Bezdetnaya L, Guillemin F, Marchal F. Bmc Cancer. 2008; 8
39. Chang E, Thekkek N, Yu WW, Colvin VL, Drezek R. Small. 2006; 2:1412. [PubMed: 17192996]
40. Nishioka Y, Yoshino H. Advanced Drug Delivery Reviews. 2001; 47:55. [PubMed: 11251245]
41. a) Oussoren C, Storm G. Pharmaceutical Research. 1997; 14:1479. [PubMed: 9358565] b) Oussoren C, Zuidema J, Crommelin DJA, Storm G. Biochimica Et Biophysica Acta-Biomembranes. 1997; 1328:261.
42. Klajnert B, Bryszewska M. Acta Biochimica Polonica. 2001; 48:199. [PubMed: 11440170]
43. a) Svenson S. European Journal of Pharmaceutics and Biopharmaceutics. 2009; 71:445. [PubMed: 18976707] b) Yang WJ, Cheng YY, Xu TW, Wang XY, Wen LP. European Journal of Medicinal Chemistry. 2009; 44:862. [PubMed: 18550227] c) Joshi N, Grinstaff M. Current Topics in Medicinal Chemistry. 2008; 8:1225. [PubMed: 18855707] d) Villalonga-Barber C, Micha-Screttas M, Steele BR, Georgopoulos A, Demetzos C. Current Topics in Medicinal Chemistry. 2008; 8:1294. [PubMed: 18855710]
44. Tomalia DA. Macromolecular Symposia. 1996; 101:243.
45. Hawker CJ, Frechet JMJ. Journal of the American Chemical Society. 1990; 112:7638.
46. Kobayashi H, Kawamoto S, Choyke PL, Sato N, Knopp MV, Star RA, Waldmann TA, Tagaya Y, Brechbiel MW. Magnetic Resonance in Medicine. 2003; 50:758. [PubMed: 14523962]
47. Kobayashi H, Kawamoto S, Bernardo M, Brechbiel MW, Knopp MV, Choyke PL. Journal of Controlled Release. 2006; 111:343. [PubMed: 16490277]
48. Talanov VS, Regino CAS, Kobayashi H, Bernardo M, Choyke PL, Brechbiel MW. Nano Letters. 2006; 6:1459. [PubMed: 16834429]
49. a) Koyama Y, Talanov VS, Bernardo M, Hama Y, Regino CAS, Brechbiel MW, Choyke PL, Kobayashi H. Journal of Magnetic Resonance Imaging. 2007; 25:866. [PubMed: 17345640] b) Kobayashi H, Koyama Y, Barrett T, Hama Y, Regino CAS, Shin IS, Jang BS, Le N, Paik CH, Choyke PL, Urano Y. Acs Nano. 2007; 1:258. [PubMed: 19079788]

50. Kobayashi H, Ogawa M, Kosaka N, Choyke PL, Urano Y. Nanomedicine. 2009; 4:411. [PubMed: 19505244]
51. Kaminskas KJ, McLeod VM, Kelly BD, Karellas P, Porter CJ. Journal of Control Release. 2009 (in Press).
52. Kim J, Chung KH, Lee CM, Seo YS, Song HC, Lee KY. Journal of Microbiology and Biotechnology. 2008; 18:1599. [PubMed: 18852518]
53. Takakura Y, Takagi A, Hashida M, Sezaki H. Pharmaceutical Research. 1987; 4:293. [PubMed: 2470072]
54. Cai S, Xie YM, Bagby TR, Cohen MS, Forrest ML. Journal of Surgical Research. 2008; 147:247. [PubMed: 18498877]
55. Hawley AE, Illum L, Davis SS. Febs Letters. 1997; 400:319. [PubMed: 9009222]
56. Dunne AA, Boerner HG, Kukula H, Schlaad H, Wiegand S, Werner JA, Antonietti M. Anticancer Research. 2007; 27:3935. [PubMed: 18225553]
57. Liu J, Meisner D, Kwong E, Wu XY, Johnston MR. Cancer Research. 2009; 69:1174. [PubMed: 19176391]
58. Kumanohoso T, Natsugoe S, Shimada M, Aikou T. Cancer Chemotherapy and Pharmacology. 1997; 40:112. [PubMed: 9182831]
59. Liu J, Wong HL, Moselhy J, Bowen B, Wu XY, Johnston MR. Lung Cancer. 2006; 51:377. [PubMed: 16413084]
60. Yang D, Yang F, Hu JH, Long J, Wang CC, Fu DL, Ni QX. Chemical Communications. 2009:4447. [PubMed: 19597621]
61. McDevitt MR, Chattopadhyay D, Kappel BJ, Jaggi JS, Schiffman SR, Antczak C, Njardarson JT, Brentjens R, Scheinberg DA. Journal of Nuclear Medicine. 2007; 48:1180. [PubMed: 17607040]
62. Murakami T, Sawada H, Tamura G, Yudasaka M, Iijima S, Tsucbida K. Nanomedicine. 2008; 3:453. [PubMed: 18694307]
63. Shimada M, Natsugoe S, Aikou T. Anticancer Research. 1995; 15:109. [PubMed: 7537484]
64. Hagiwara A, Takahashi T, Iwamoto A, Yoneyama C, Matsumoto S, Muranishi S. Anti-Cancer Drugs. 1991; 2:261. [PubMed: 1802020]
65. Hagiwara A, Ahn T, Ueda T, Iwamoto A, Ueda T, Torii T, Takahashi T. Anticancer Research. 1986; 6:1005. [PubMed: 2432828]

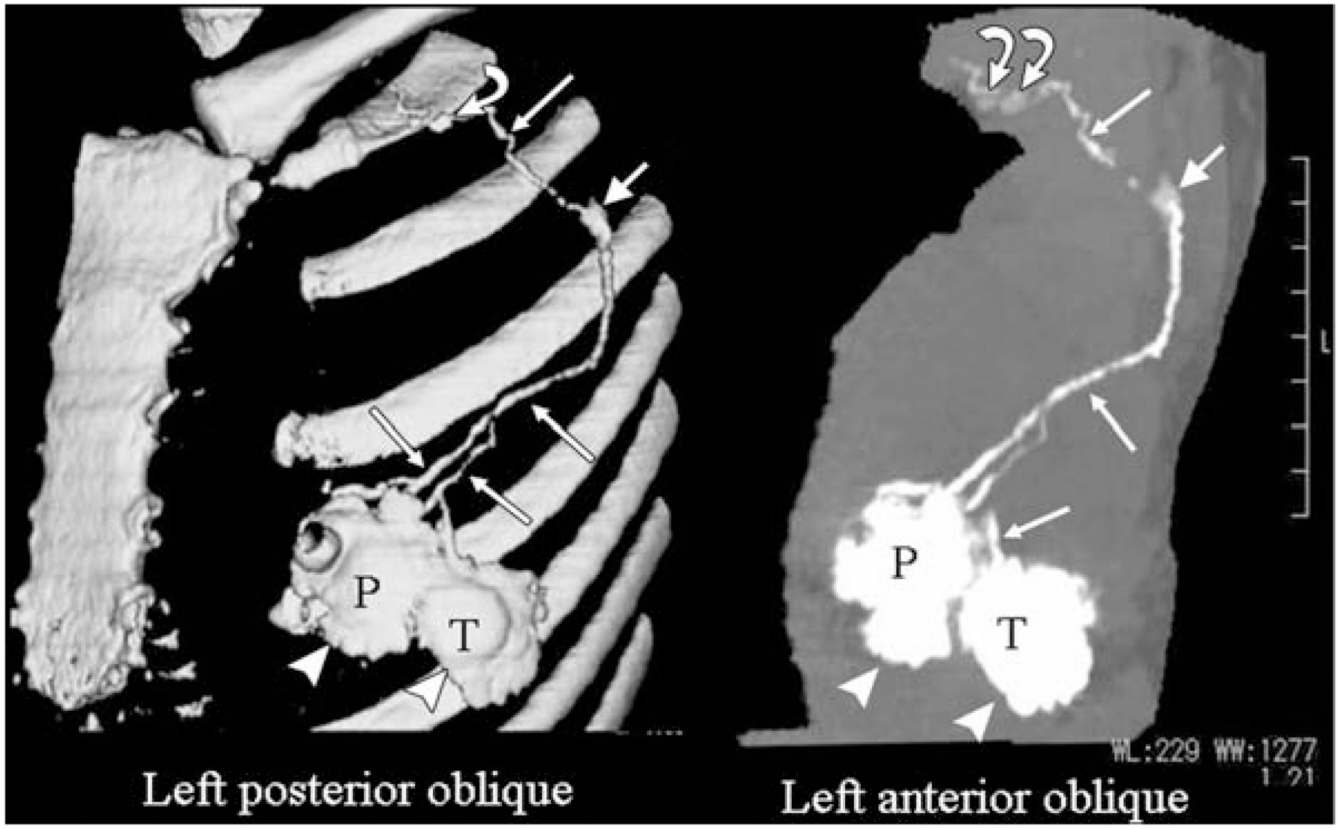

Fig 1.
CT image illustrating the lymphatic pathways enhanced with injected iopamidol.[14]

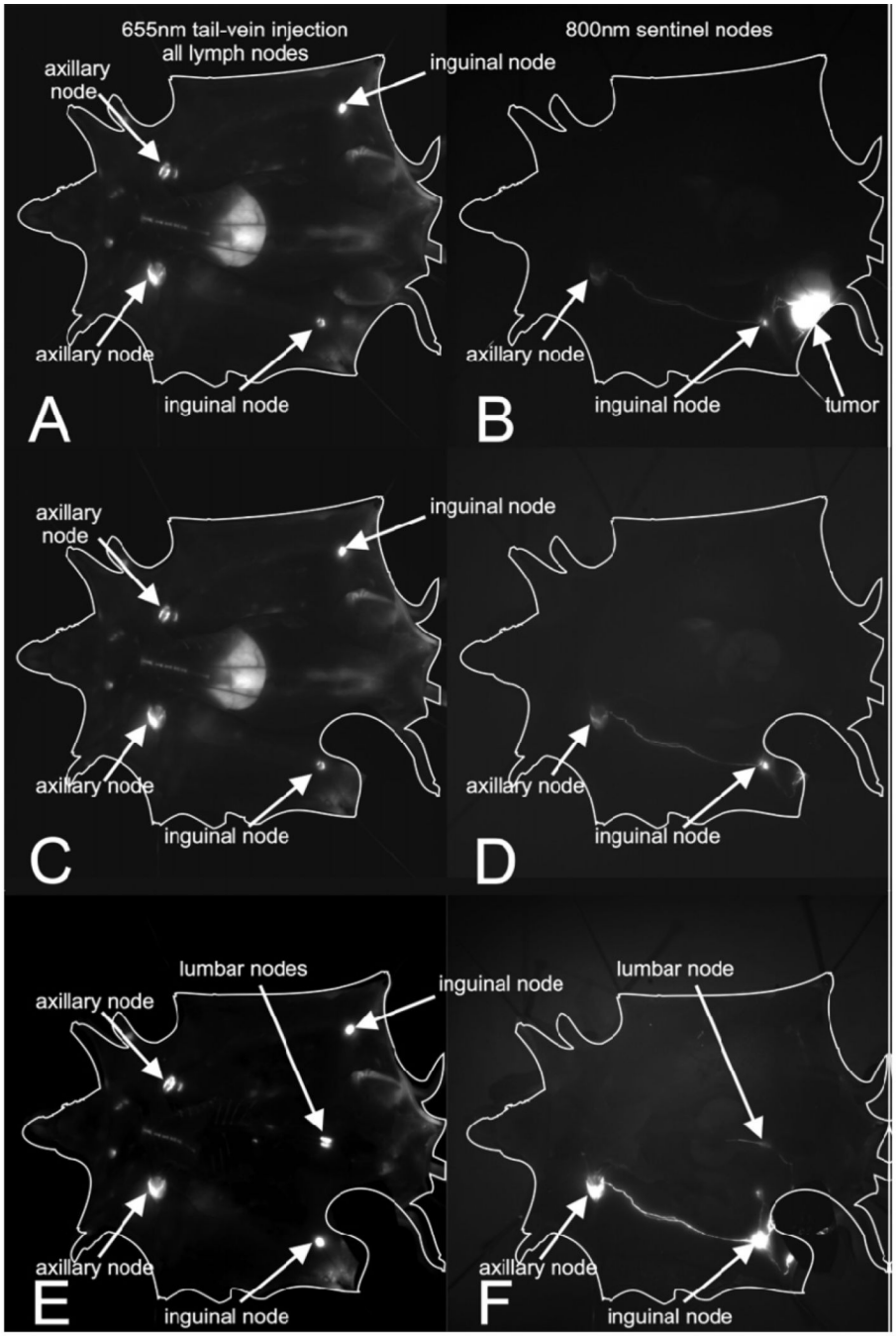

Fig 2.

Fluorescent imaging lymphatic drainage after injection of fluorescent QDs into mice bearing M21 melanoma. Left frames A,C,E: channel after tail vein injection of PEG 5k-COOH coated QDs; right frames B,DE: 800-nm channel after intratumoral injection of PEG 5k-OMe coated QDs.[35]

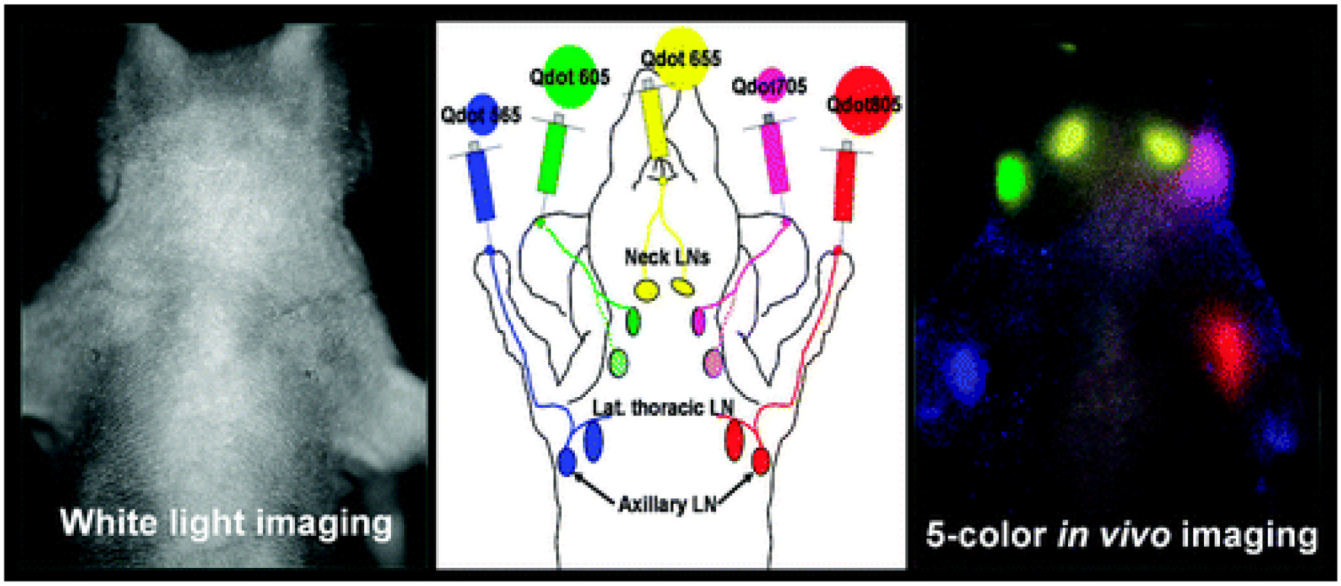

Fig 3.
Illustration of simultaneous multicolor imaging of lymphatic drainage[36a]

Table 1

Size analysis of five QDS studied

QDs/methods	QD 565 (Cd/Se)	QD 605 (Cd/Se)	QD 655 (Cd/Se)	QD 705 (Cd/Te)	QD 800 (Cd/Te)
DLS[a] (diameter in nm)	15.0 ± 6.0	15.4 ± 4.3	ND[1]	ND[1]	16.9 ± 7.3
TEM[b] (diameter in nm)	7.8 ± 0.5	10.3 ± 0.5	13.4 ± 0.7	9.7 ± 0.3	12.0 ± 0.5
HPLC[c] elution time (min)	17.24 ± 0.01	17.01 ± 0.01	16.85 ± 0.01	16.97 ± 0.01	16.85 ± 0.00
diameter (nm)	(16.3 nm)	(17.1 nm)	(18.9 nm)	(18.0 nm)	(18.8 nm)

[a] Not determined: data is not reliable because of the fluorescence contamination in the signal.

[b] TEM: sizes of well-separated 50 particles in each sample were measured.

[c] Standard proteins: IgM (24.2 nm); 16.08 ± 0.00, thyroglobulin; (17.0 nm); 17.11 ± 0.01 min, IgG (11.0 nm); 18.17 ± 0.00 min.

Adv Drug Deliv Rev. Author manuscript; available in PMC 2012 September 10.